

A Prototype of a Fully-Implantable Charge-Balanced Artificial Sensory Stimulator for Bi-directional Brain-Computer-Interface (BD-BCI)

Won J. Sohn¹, Po T. Wang², Spencer Kellis^{3,4}, Richard A. Andersen³, Charles Y. Liu⁴, Payam Heydari⁵, Zoran Nenadic^{2,5}, and An H. Do¹.

Abstract—Bi-directional brain-computer interfaces (BD-BCI) to restore movement and sensation must achieve concurrent operation of recording and decoding of motor commands from the brain and stimulating the brain with somatosensory feedback. Previously we developed and validated a benchtop prototype of a fully implantable BCI system for motor decoding. Here, a prototype artificial sensory stimulator was integrated into the benchtop system to develop a prototype of a fully-implantable BD-BCI. The artificial sensory stimulator incorporates an active charge balancing mechanism based on pulse-width modulation to ensure safe stimulation for chronically interfaced electrodes to prevent damage to brain tissue and electrodes. The feasibility of the BD-BCI system’s active charge balancing was tested in phantom brain tissue. With the charge-balancing, the removal of the residual charges on an electrode was evident. This is a critical milestone toward fully-implantable BD-BCI systems.

Clinical Relevance— For a chronically implanted BD-BCI system, additional charge-balancing considerations are required to prevent charge accumulation and potential tissue/electrode damage. This study demonstrates a safe electrocortical stimulation method which integrates into the existing benchtop system for a full-implantable BD-BCI interface.

I. INTRODUCTION

Brain-computer-interfaces (BCI) represent a promising means to restore brain control of external devices after neurological injuries. A BCI recognizes the motor intent of the user through the brain signal to operate neuroprosthetics which could ultimately enable activities of daily living such as self-feeding and walking again toward functional independence. For people suffering from a severe neurological impairment, the technology has shown considerable promise to bypass the damaged spinal cord by decoding motor intentions from outgoing brain signals [1, 2].

While much BCI research has been conducted on motor control of robotic limbs, there has been little work on how to provide sensory feedback to the patient. Since the loss of somatosensation causes severe deficits in motor control [3-5], electrically stimulating the somatosensory cortex (S1) to artificially evoke tactile and proprioceptive percepts [6, 7] can be a promising approach to restore sensation to patients with paralysis. Although there have been pioneering works

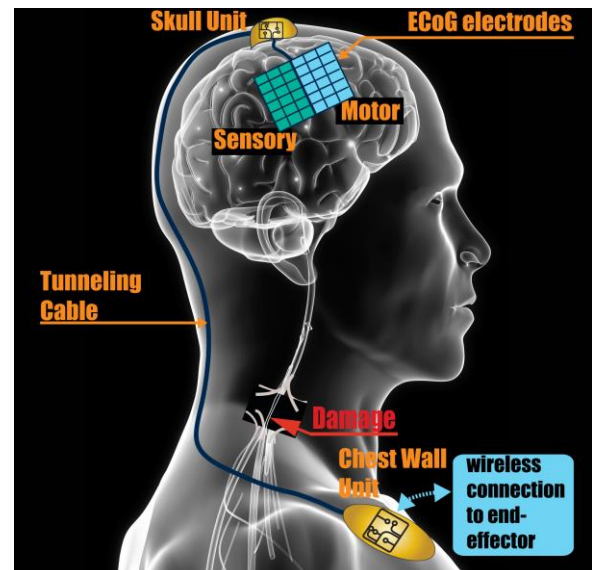


Fig.1. Envisioned fully-implantable BD-BCI system. This illustrates a hypothetical scenario where a person with a cervical spinal cord injury (SCI) is implanted with the skull unit (SU) and chest wall unit (CWU) connected by a tunneling cable to bypass the damaged sensorimotor pathway. ECoG electrodes are implanted over the sensory and motor cortex which map to the sensorimotor fields relevant to desired tasks, e.g. walking. The SU will amplify, multiplex, and digitize the motor ECoG signals and pass them to the CWU, which sends commands to the end-effector. The movement of the end-effector will trigger the electrical stimulator in CWU to send current pulses to the sensory ECoG grids to elicit artificial somatosensation of the movement.

investigating the impact of artificial sensory stimulation as a feedback in the control of upper-limb prosthetic devices in a controlled lab setting [6, 8-10], there is no fully-implantable BCI system providing artificial sensation through direct cortical stimulation intended for chronic use in human.

We envision to address the need for a closed-loop fully implantable bi-directional BCI (BD-BCI) (Fig. 1), where electrocorticogram (ECoG) electrode grids will serve as the platform for motor signal acquisition and sensory cortex stimulation. Unlike EEG, ECoG signals have high spatiotemporal resolution (\sim mm, \leq 200 Hz) and signal-to-noise ratio (SNR), and are resistant to motion artifacts [11]. In addition, ECoG grids are safe for permanent implantation with >5 yrs of demonstrated signal stability [12]. Permanent ECoG

Supported by National Science Foundation (Award #1646275)

¹Dept. of Neurology, UCI, Irvine, CA 92697, wonjsohn@gmail.com, and@uci.edu.

²Dept. of Biomedical Engineering, University of California Irvine (UCI), Irvine, CA 92697, ptwang@uci.edu, znenadic@uci.edu.

³Div. of Biology and Biological Engineering, CALTECH, Pasadena, CA

91125, andersen@vis.caltech.edu

⁴Dept. of Neurological Surgery, University of Southern California, Los Angeles, CA 90033, cliu@usc.edu

⁵Dept. of Electrical Engineering and Computer Science, UCI, Irvine, CA 92697, payam@uci.edu

implantation also obviates the need for (dis)mounting procedures and may eliminate external electronics, thereby making ECoG an aesthetically and socially acceptable BCI platform.

Toward this vision, we already developed and tested a benchtop of a fully-implantable unidirectional BCI system that can decode motor commands from ECoG signals [13]. However, the sensory feedback component is still completely absent. As a step toward the fully implantable BD-BCI, an electrocortical stimulator must be integrated with the existing unidirectional BCI system [13]. To achieve seamless integration, it is necessary to have precision-control of the stimulation parameters operating concurrently with the downstream motor decoding while keeping the small footprint. Furthermore, additional considerations are required for chronically interfaced electrodes to prevent mechanisms from damaging tissue and the electrodes [14]. Specifically, due to manufacturing process variation and mismatch in anode and cathode electrode impedances, the pulse generating circuit cannot guarantee charge neutrality of the bi-phasic stimulation signal. It is specifically important for stimulation in the chronically interfaced electrode to provide active charge-balancing in order not induce irreversible reduction and oxidation reaction that can lead to electrode degradation and tissue damage [14]. In this study, we describe the design of the BD-BCI via integration of the unidirectional BCI with a stimulation circuit, as well as basic benchtop validation of the stimulation and charge balancing capability.

II. METHODS

A. Development and Integration of the Programmable Stimulator in the Existing Benchtop BCI system

We developed a customized stimulator to be integrated into the previously developed benchtop system for a fully-implantable BD-BCI interface [13]. To this purpose, the stimulator was designed to *share* one of the two existing microcontroller cores to generate precise pulse-width-modulated waveforms by utilizing the Timer/Counter for Control Applications (TCC) module of the microcontroller. In this way, the stimulator is immune to processing delays because of the independent operation of the TCC which minimizes interruptions to ongoing ECoG signal acquisition and motor decoding. In order to elicit artificial sensation, the design aimed at achieving a maximum stimulation current of 15 mA to be delivered across 1.0 k Ω load (a typical electrode impedance above somatosensory cortex is <600 Ω between

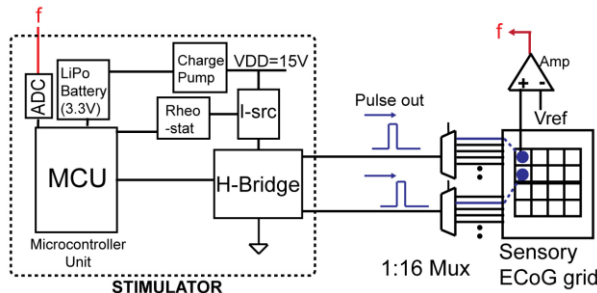


Fig.2. Schematic of the stimulator circuit. The output pulses are current-controlled, biphasic pulses with programmable pulse width, pulse frequency, and charge density. MCU: microcontroller. ADC: analog-to-digital converter. I-src: current source. Vref: reference voltage. Mux: Multiplexer. f: feedback voltage.

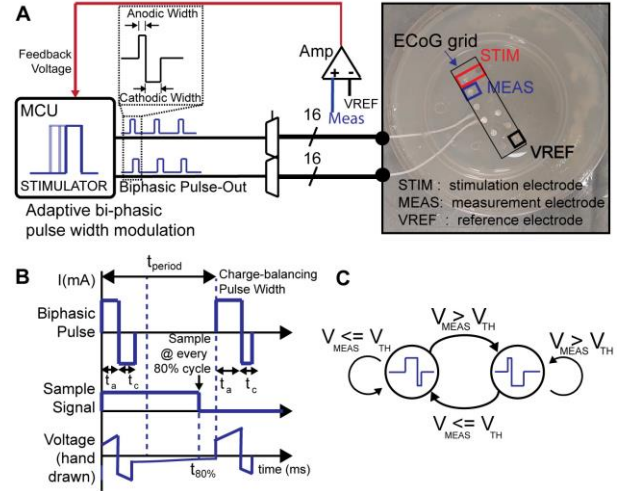


Fig.3. A. Schematic of the active charge-balancing circuit. The increased voltage at measurement electrode (V_{MEAS}) activates the adaptive removal of residual charges by pulse width-modulated correction. Right box: ECoG grid is placed on phantom brain tissue. Dipole channels in 6x2 ECoG grid are stimulated bipolarly. Charge accumulation was tracked in the neighboring electrode from the stimulation pairs. The reference voltage was defined from the most distant electrode in the grid. B. Illustration of a biphasic pulse waveform and the timing of the voltage measurement (V_{MEAS}). C. Binary state machine algorithm to test the active charge balancing. The output of each state differs in their ratio between the anodic and cathodic pulse width (either 12:1 or 1:12). V_{TH} : pre-configured threshold voltage.

two neighboring channels [15]) therefore supply voltage as high as 15V is required. From the 3.3V supply from a LiPo battery, such high VDD is provided by incorporating cascaded charge-pump circuits (Maxim Integrated, San Jose, CA) (Fig. 2). Similar to the stimulator in [16], a current-controlled biphasic square pulse stimulation is implemented with H-bridge (Texas Instruments, Dallas, TX) driven by a current source (Nexperia, Nijmegen, Netherlands), which is controlled with a digital rheostat (Maxim Integrated, San Jose, CA). The stimulation parameters (pulse width, pulse frequency, charge density) are precision-controlled by a programmable microcontroller (Microchip, Chandler, AZ). The system can deliver stimulation with pulse frequency up to 1 kHz, pulse width resolution of 10 ns, and arbitrary train duration. Two 16-to-1 analog multiplexers (Analog Devices, Norwood, MA) select channels in the ECoG grid for bipolar stimulation. The measured feedback voltage is amplified (Texas Instruments, Dallas, TX) and digitally converted to be read by the ADC pin of the microcontroller. ADC detects the voltage off-set as small as 1mV.

B. Experiment on Charge-Balancing Methodology

To deliver a current pulse to the chronically interfaced electrodes, a pulse-width modulated charge-balancing algorithm is implemented to prevent damages in the tissue and the electrodes. Specifically, sampled voltages at each pulse cycle will be used as a feedback signal to adjust the anodic and cathodic pulse-widths of the immediate next pulse cycle depending on the level of measured voltage in reference to the preconfigured threshold (Fig. 3A, B).

The function of charge-balancing is tested by 1) an intentional build-up of residual charges at the measuring electrode and 2) activating the active charge-balancing circuit to assess the removal of the accumulated charges. To test the

functional validity of the proof-of-concept active charge-balancing, a binary state machine modulating the pulse-width of the output stimulation was implemented as in Fig. 3C, which operates on the arbitrarily set threshold of 80 mV. The stimulator outputs the reversal of the default asymmetric biphasic waveform (anodic to cathodic ratio=1:12) when the measured voltage exceeds the threshold, and if the voltage drops below the threshold, the waveform returns to the default 12:1 waveform. It is to be noted that the algorithm only needs to correct the excess positive voltage and therefore only a single threshold is needed (as opposed to two thresholds in a typical window comparator). Due to the stimulation artifact from the stimulating dipoles, the voltage is sampled at 80% of each duty cycle (Fig. 3C) to avoid sampling the residual effect of the artifact. The transient voltage response due to the switching of the biphasic waveform and the steady-state voltage with and without the active charge-balancing was measured and characterized.

To prepare the environment to test the charge-balancing, a phantom to mimic brain tissue was first prepared with food-grade agar in a Petri dish as in [17], and a thin layer of 1x phosphate buffered saline (PBS) which was poured on top. A standard 6x2 ECoG grid (Ad-Tech, Oak Creek, WI) with platinum electrodes (4 mm diameter, 2.3 mm exposed diameter, 10 mm pitch) delivered currents at the stimulating dipoles (Fig. 3A), and the voltage was recorded by a data acquisition system (Biopac System, Inc. Goleta, CA) with sampling frequency of 20 kHz. The measured impedance between the stimulating dipoles was 2.0 k Ω at 30 Hz, which limits the maximum current to 7.5 mA. The farthest electrode in the grid from the stimulating dipole was designated as the reference (V_{REF}), to which the measured voltage is referenced.

III. RESULTS

The stimulator circuit was successfully implemented on the printed circuit board (PCB) which integrates the stimulator and the existing BCI system from [13] (Fig. 4). The output stimulation generated asymmetric biphasic square pulses which are parameter-controlled in the charge-balancing experiment. Fig. 5A shows the transient voltage response at the measurement electrode according to the change in the biphasic pulse-width profile to demonstrate the effect of pulse-width modulation. Without any adaptive algorithm, the 12-to-1 anodic vs cathodic pulse resulted in a steady-state positive

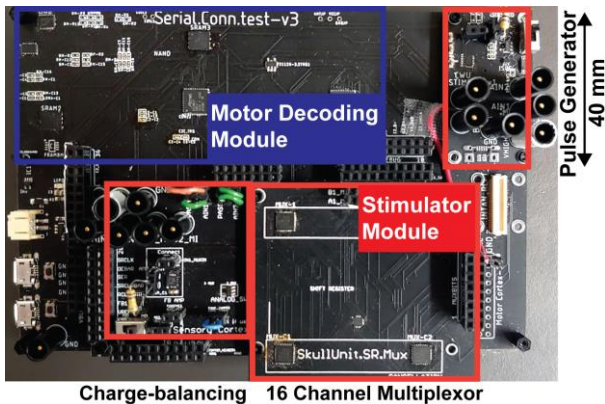


Fig. 4. Stimulator module integrated into the existing benchtop design for a fully-implantable BD-BCI interface. This development board includes expansion pin-outs for debugging which will be removed in the final miniaturized design.

potential. An abrupt switch to 1-to-12 anodic vs cathodic pulse caused the transient reversal of the steady-state voltage to negative as expected. Fig. 5B shows the effect of the active charge-balancing in removing residual charges on an electrode. When the charge-balancing is off, the steady-state voltage was 0.315 ± 0.048 V, whereas it was -0.012 ± 0.052 V when the charge-balancing mechanism was engaged. Fig. 5B displays 900 sampled data points for each condition to contrast the steady-state voltages between the two conditions. The accumulation of charge at the electrode by 12:1 waveform at 200Hz is reflected in 0.315 V increase. The net charge per phase for the 750 μ s: 62.5 μ s anodic:cathodic phase was 5.16 μ C/phase.

IV. DISCUSSION

The current study tests the feasibility of an artificial stimulator equipped with pulse-width modulated active charge-balancing, which is developed and integrated into the previously developed benchtop motor decoding system for a fully-implantable BD-BCI interface [13]. The developed stimulator in the integrated benchtop system demonstrates that the active charge-balancing method is capable of effectively removing the residual charges on an electrode to achieve charge neutrality to prevent mechanisms from damaging tissue and the electrodes.

The parameters for biphasic pulse-widths used for the charge-balancing test were intentionally set to an extreme to demonstrate the build-up and removal of the residual charges in a relatively short time period. This generated a scenario where the charge-balancing effect can be evident. Typically, a shorter pulse width (<200 μ s) and symmetric biphasic pulses are used which reduce the net charge per phase to meet the FDA's recommended safety limit of 25 μ C/cm²/phase [18]. The max current capacity of 7.5 mA from the phantom tissue is expected to reach 15 mA since we expect the impedance of the surface of ECoG electrode-tissue interface to be near 1.0 k Ω [15]. However, the current capacity will be sufficient since the current of 3 mA marked the threshold at which most participants (67%) reported a sensation [19].

A limitation of the study is that the effect of stimulation artifact on the performance of the simultaneous BCI motor

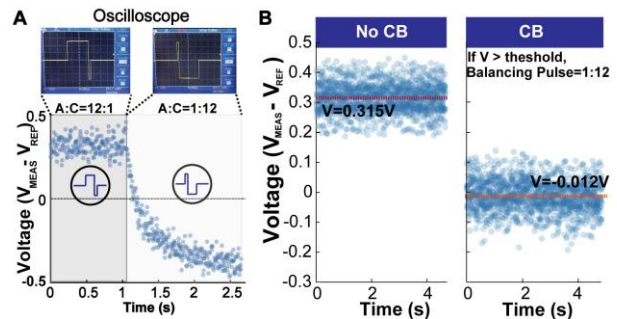


Fig. 5. A. Transient voltage response at the measurement electrode to the switching of the pulse output profile without the charge balancing mechanism: 1) Anodic vs Cathodic =12:1, 2) Anodic vs Cathodic=1:12. B. The effect of charge-balancing. Measured steady-state voltage is 0.315 ± 0.048 when there is no charge-balancing, and -0.012 ± 0.052 when there is active charge balancing. The voltage is measured once per each cycle as in Fig. 3B. CB: Charge-Balancing. *Each dot represents a voltage sample taken at 80% of each duty cycle of the 200 Hz pulse train.

decoding is not assessed. However, it is expected that techniques to suppress stimulation artifacts [20-22] will mediate the problem. Future work includes testing to determine if the stimulation output is equivalent to FDA-approved cortical stimulators (e.g. Natus Nicolet® Cortical Stimulator, Natus Medical, Inc., Pleasanton, CA), followed by testing the quality of the artificial sensation in human subjects elicited by encoding movements of the end-effectors. Miniaturization of the system to an implantable form factor will also be pursued.

V. CONCLUSION

The current study achieves a step toward a fully-implantable BD-BCI by integrating a prototype artificial sensory stimulator into the existing unidirectional BCI system. We demonstrated that system can charge-balance electrical stimulation across ECoG electrodes to ensure safe stimulation for both the brain tissue and the electrodes.

ACKNOWLEDGMENT

This study was supported by NSF grant #1646275.

REFERENCES

- [1] A. R. Donati, S. Shokur, E. Morya, D. S. Campos, R. C. Moioli, C. M. Gitti, *et al.*, "Long-Term Training with a Brain-Machine Interface-Based Gait Protocol Induces Partial Neurological Recovery in Paraplegic Patients," *Sci Rep*, vol. 6, p. 30383, Aug 11 2016.
- [2] M. A. Lebedev and M. A. Nicolelis, "Brain-Machine Interfaces: From Basic Science to Neuroprostheses and Neurorehabilitation," *Physiol Rev*, vol. 97, Apr 2017.
- [3] J. C. Rothwell, M. M. Traub, B. L. Day, J. A. Obeso, P. K. Thomas, and C. D. Marsden, "Manual motor performance in a deafferented man," *Brain*, vol. 105 (Pt 3), pp. 515-42, Sep 1982.
- [4] R. L. Sainburg, H. Poizner, and C. Ghez, "Loss of proprioception produces deficits in interjoint coordination," *J Neurophys*, vol. 70, pp. 2136-47, Nov 1993.
- [5] J. Gordon, M. F. Ghilardi, and C. Ghez, "Impairments of reaching movements in patients without proprioception. I. Spatial errors," *J Neurophys*, v. 73, pp. 347-60, Jan 1995.
- [6] G. A. Tabot, S. S. Kim, J. E. Winberry, and S. J. Bensmaia, "Restoring tactile and proprioceptive sensation through a brain interface," *Neurobiol Dis*, vol. 83, pp. 191-8, Nov 2015.
- [7] J. A. Lubin, J. K. Strebe, and J. S. Kuo, "Intracortical Microstimulation of Human Somatosensory Cortex Reproduces Touch in Spinal Cord Injury Patient," *Neurosurgery*, vol. 80, pp. N29-N30, May 1 2017.
- [8] J. E. O'Doherty, M. A. Lebedev, Z. Li, and M. A. L. Nicolelis, "Virtual Active Touch Using Randomly Patterned Intracortical Microstimulation," *Ieee Transactions on Neural Systems and Rehabilitation Engineering*, vol. 20, pp. 85-93, Jan 2012.
- [9] S. N. Flesher, J. L. Collinger, S. T. Foldes, J. M. Weiss, J. E. Downey, E. C. Tyler-Kabara, *et al.*, "Intracortical microstimulation of human somatosensory cortex," *Science Translational Medicine*, vol. 8, Oct 19 2016.
- [10] B. D. Swan, L. B. Gasperson, M. O. Krucoff, W. M. Grill, and D. A. Turner, "Sensory percepts induced by microwire array and DBS microstimulation in human sensory thalamus," *Brain Stimulation*, vol. 11, pp. 416-422, Mar-Apr 2018.
- [11] T. Ball, M. Kern, I. Mutschler, A. Aertsen, and A. Schulze-Bonhage, "Signal quality of simultaneously recorded invasive and non-invasive EEG," *Neuroimage*, vol. 46, pp. 708-16, Jul 1 2009.
- [12] C. Wu, J. J. Evans, C. Skidmore, M. R. Sperling, and A. D. Sharan, "Impedance variations over time for a closed-loop neurostimulation device: early experience with chronically implanted electrodes," *Neuromodulation*, vol. 16, pp. 46-50; discussion 50, Jan-Feb 2013.
- [13] P. T. Wang, E. Camacho, M. Wang, Y. Li, S. J. Shaw, M. Armacost, *et al.*, "A benchtop system to assess the feasibility of a fully independent and implantable brain-machine interface," *J Neural Eng*, vol. 16, p. 066043, Nov 12 2019.
- [14] D. R. Merrill, M. Bikson, and J. G. Jefferys, "Electrical stimulation of excitable tissue: design of efficacious and safe protocols," *J Neurosci Methods*, vol. 141, pp. 171-98, Feb 15 2005.
- [15] S. V. Hiremath, E. C. Tyler-Kabara, J. J. Wheeler, D. W. Moran, R. A. Gaunt, J. L. Collinger, *et al.*, "Human perception of electrical stimulation on the surface of somatosensory cortex," *PLoS One*, vol. 12, 2017.
- [16] P. T. Wang, A. Karimi-Bidhendi, C. Y. Liu, Z. Nenadic, P. Heydari, and A. H. Do, "A Low-Cost, Fully Programmable, Battery Powered Direct Cortical Electrical Stimulator," *Journal of Medical Devices-Transactions of the Asme*, vol. 10, Sep 2016.
- [17] M. A. Kandadai, J. L. Raymond, and G. J. Shaw, "Comparison of electrical conductivities of various brain phantom gels: Developing a 'brain gel model'," *Materials Science & Engineering C-Materials for Biological Applications*, vol. 32, pp. 2664-2667, Dec 1 2012.
- [18] FDA, "Summary of safety and effectiveness data (SSED)," *PMA P100026*, 2019.
- [19] B. Lee, D. Kramer, M. Armenta Salas, S. Kellis, D. Brown, T. Dobreva, *et al.*, "Engineering Artificial Somatosensation Through Cortical Stimulation in Humans," *Front Syst Neurosci*, vol. 12, p. 24, 2018.
- [20] P. T. Wang, C. M. McCrimmon, P. Heydari, A. H. Do, and Z. Nenadic, "Subspace-Based Suppression of Cortical Stimulation Artifacts," *Conf Proc IEEE Eng Med Biol Soc*, vol. 2018, pp. 2426-2429, Jul 2018.
- [21] A. Zhou, B. C. Johnson, and R. Muller, "Toward true closed-loop neuromodulation: artifact-free recording during stimulation," *Curr Opin Neurobiol*, vol. 50, pp. 119-127, Jun 2018.
- [22] J. Lim, P. T. Wang, H. R. Pu, C. Y. Liu, S. Kellis, R. A. Andersen, *et al.*, "Dipole Cancellation as an Artifact Suppression Technique in Simultaneous Electroencephalography Stimulation and Recording," *2019 9th International Ieee/Embs Conference on Neural Engineering (Ner)*, pp. 725-729, 2019.